2024 IEEE International Conference on Robotics and Automation (ICRA 2024)
May 13-17, 2024. Yokohama, Japan

A Movable Microfluidic Chip with Gap Effect for Manipulation of Oocytes

Shuzhang Liang, Satoshi Amaya, Hirotaka Sugiura, Hao Mo, Yuguo Dai, and Fumihito Arai *Member, IEEE*

Abstract— **This study proposes a novel movable microfluidic chip in which a microfluidic chip is integrated into a robotic manipulator for manipulating oocytes. The microfluidic device has the ability to release a single oocyte with a gap effect. The robotic manipulator can control the position of the microfluidic chip. The microfluidic chip with a pipette tip is directly fabricated using 3D printing. *Xenopus* oocyte was used in the experiment. When oocytes move from the back side of the channel to the front side, they generate gaps between each other. The gap distance can reach about 16 times the diameter of the oocyte. In addition, a capacitive sensor was used to detect oocytes in the manipulation processes. The results showed that oocytes were successfully released one by one with no deformation in shape using the movable microfluidic chip. The method has significant advantages in biomedicine engineering and micro-nano-manipulation.**

I. Introduction

Recently, single-cell processes have become key points in biological engineering, such as gene expression [1], [2], proteomic analysis, and detection of ion channels on cell membranes [3]. To analyze a single cell, it is first necessary to manipulate one cell from the cell population. There are usually different methods to manipulate the cells [4], [5], which contain contact and non-contact methods. Generally, non-contact methods are convenient for manipulation. For example, magnetic tweezers control macrophage cells for tumor therapy [6]. Acoustofluidics device is used for cell perforation [7]. Optical tweezers are applied to manipulate microorganisms [8]. These techniques both exploit an external field. The system is complex, and it is not easy to manipulate large-size particles. As for contact manipulation, it can provide a large manipulating force because the contact method manipulates cells directly. For example, a microrobot is considered integrated into microfluidic chips [9] because the microrobot can achieve physical/chemical interaction by motion. An on-chip robot, proposed by M. Hagiwara et al. [9], has been successfully used for sorting and delivering oocytes. S. Sakuma et al. [10] also applied a robot-integrated microfluidic chip to continuously measure the mechanical properties of single spheroids. Furthermore, a ferrofluid-robot [11] was used for automated microfluidic logistics for flexible manipulation. In these cases, since the microfluidic environment is closed, it is not easy to put the microrobot into the microfluidic chip. To build the flexible cell operating system, an open microfluidic chip [12], [13], combined with a glass pipette, was conducted for manipulation. Meanwhile, glass pipettes can be used for other applications, such as rotation and RNA injection.

Among these technologies, microfluidic chips are a simple and low-cost method [14]. It only needs to design a specific structure in the channel to achieve different flow effects. Therefore, microfluidic devices have been widely applied for cell manipulation [15], [16]. In microfluidic chips, cells are typically manipulated using inertial effects [17], microstructure in channels [18], multiple phase fluids [19], and other physical fields [20]. For example, D. Lv et al. [21] described a microfluidic chip that the capture efficiencies/release efficiencies of single cells were 91.34% /93.67%. It achieved a high throughput separation. Y. Kasai et al. [22] presented a novel on-chip sorting method to select large-size (>100 micrometers) particles. S. Liang et al. [23] demonstrated a versatile optoelectronic microfluidic system that can freely manipulate different shapes of micro-objects with virtual patterns. These devices have many advantages, such as easy fabrication, integration, good biocompatibility, stability, and high throughput. Even some microfluidic chips have already been developed into commercial products, such as flow cytometry [24]. However, in the single-cell process, it requires transporting cells from one location to another for analysis. These traditional microfluidic chips are usually fixed to the system and cannot be used for interacting operations. It limits the microfluidic chip's ability to achieve more flexible cell processing.

Here, we present a movable microfluidic chip method for manipulating cells, as shown in Fig. 1. A microfluidic chip with a simple structure is designed and integrated into a 3DoF robot manipulator. To achieve single-cell manipulation, we analyzed the flow model based on flow characteristics in the channel. The finite element method is applied to simulate the velocity effect. The device has a pipette tip and is fabricated directly by 3D printing. We use the *Xenopus* oocyte to evaluate the manipulation ability of the movable microfluidic chip. The microfluidic chip can generate a gap effect between oocytes. Moreover, a capacitive sensor is used to detect the oocyte signals for controlling the pump. The robotic manipulator controls the position of the microfluidic chip. The tip position accuracy is determined by the manipulator. Finally, we

*This work was supported by JST Moonshot R&D – MILLENNIA Program Grant Number JPMJMS2033-08. We thank the Chinese Scholarship Council for supporting the author S. LIANG in his Ph.D. study.

Shuzhang Liang (e-mail: liang-shuzhang589@g.ecc.u-tokyo.ac.jp), Satoshi Amaya (e-mail: amaya@mesl.t.u-tokyo.ac.jp), Hirotaka Sugiura (e-mail: hsugiura965@g.ecc.u-tokyo.ac.jp), Hao Mo (e-mail: mohao1814@g.ecc.u-tokyo.ac.jp), Yuguo Dai (e-mail: daiyuguo5612@g.ecc.u-tokyo.ac.jp), is with Department of Mechanical Engineering, The University of Tokyo, Tokyo 113-8656, Japan.

Fumihito Arai is with Department of Mechanical Engineering, The University of Tokyo, Tokyo 113-8656, Japan (e-mail: araifumihito@g.ecc.u-tokyo.ac.jp).

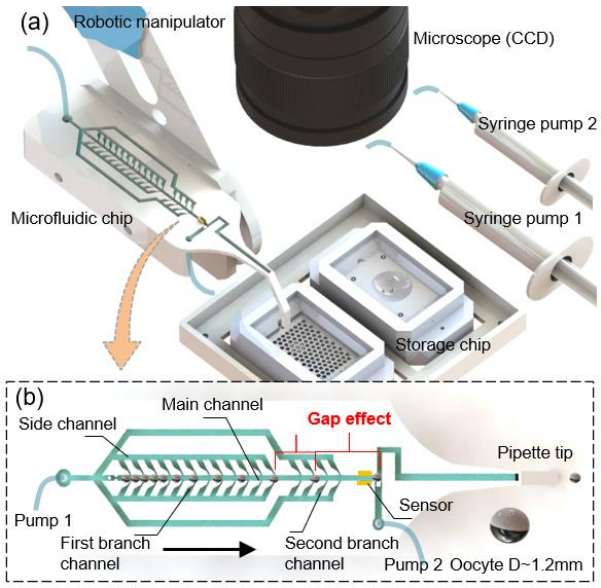

Fig. 1. Conceptual overview of a movable microfluidic chip for manipulation of oocytes. (a) Schematic configuration of the movable microfluidic chip. (b) A gap effect in the microfluidic chip.

demonstrate the movable microfluidic chip to manipulate single oocytes. The proposed method has the advantage of flexible and automated cell engineering.

II. METHOD

A. Flow distribution and simulation of the microfluidic chip

Since cell analysis processes usually require the isolation of a single cell, we consider a microfluidic chip capable of manipulating a single cell. Although there are many microfluidic devices for separating cells, the design is complex [25]. These devices utilize the microstructure and may cause damage to cells due to the impact between the cells and the structures. Here, a simple microfluidic chip is designed to achieve cell separation, as shown in Fig. 1(b). The device consists of a main channel, first branch channel part, second branch channel part, side channel, a pipette tip, and two pump connection ports. The cells only move in the main channel without any obstacles. It utilizes only the flow velocity property in the channel to manipulate cells. The cell is dragged with hydrodynamic force F_d [26].

$$F_d = \Delta p / R \tag{1}$$

Where, R is the flow resistance, and Δp is the drop pressure in the channel. To evaluate the flow model, an equivalent hydraulic circuit is established to analyze the velocity [10], as shown in Fig. 2(a). Considering the symmetrical structure of the microfluidic chip, a half model is used for depiction. Here, the structure of the channel is divided into $n+1$ parts. In the flow-driving channel, with Hagen-Poiseuille's law [26], the pressure drop, hydraulic resistance, and flow rate of one part can be expressed as:

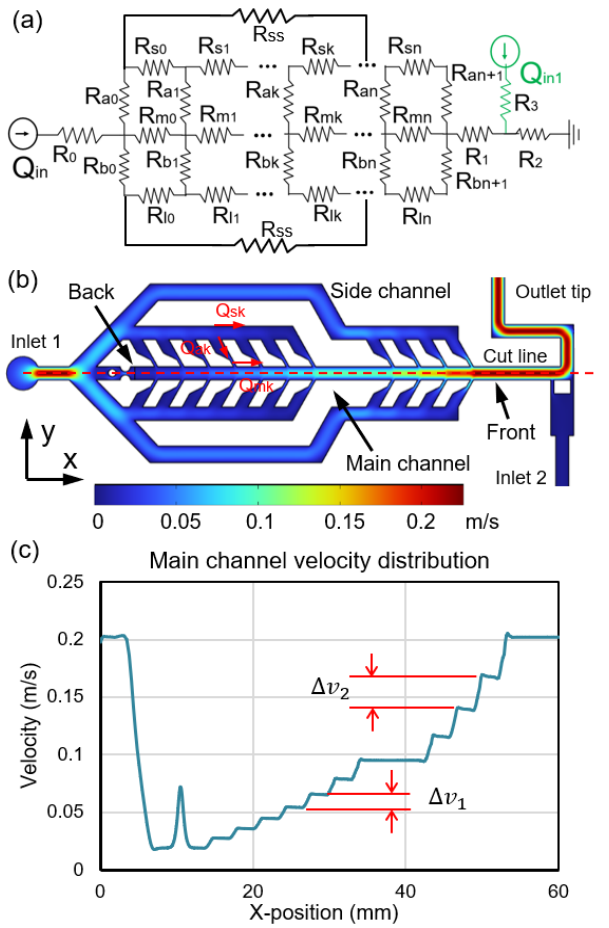

Fig. 2. Theoretical analysis of flow in the channel. (a) Schematic diagram of the equivalent hydraulic circuit. (b) Simulation of flow distribution. (c) The velocity of flow in the main channel (red cut line).

$$\begin{cases} Q_{m0}R_{m0} = Q_{a0}R_{a0} + Q_{a1}R_{a1} + Q_{s0}R_{s0} \\ Q_{ak}R_{ak} + Q_{mk}R_{mk} = Q_{ak+1}R_{ak+1} + Q_{sk}R_{sk} \\ Q_{an}R_{an} + Q_{mn}R_{mn} = Q_{an+1}R_{an+1} + Q_{sn}R_{sn} \end{cases} \tag{2}$$

Where, Q_{ak}, Q_{mk}, and Q_{sk} are the flow rate of the branch channel, main channel, and side channel, respectively. R_{ak}, R_{mk}, and R_{sk} are the flow resistance of the branch channel, main channel, and side channel, respectively.

In addition, according to the continuity of fluid in the channel, we can obtain the relationship as follows:

$$Q_{sk} = Q_{ak+1} + Q_{sk+1} \tag{3}$$

$$Q_{mk} = Q_{ak} + Q_{mk-1} \tag{4}$$

In this case, the branch channels are the same size, and the distance between each branch channel is also the same. Thus, $R_{ak} = R_{ak+1}$, and $R_{sk} = R_{mk}$ are obtained from the hydraulic resistance equation of a rectangular microchannel [27]. Due to the design of a narrow channel to connect the branch channel to the main channel, $R_{sk} < R_{ak}$. We obtain $Q_{sk+1} > Q_{ak+1}$. It means that there is more flow through the side channel than the branch channel. $Q_{ak+1} > Q_{ak}$ shows that the front branch channel has a higher flow rate. From Eqs. (2), (3) and (4), $(Q_{ak} - Q_{ak+1})(R_{ak} + R_{mk}) = (Q_{sk+1} - Q_{mk-1})R_{mk}$. Finally, $Q_{mk+1} > Q_{mk}$ and solution flow into the

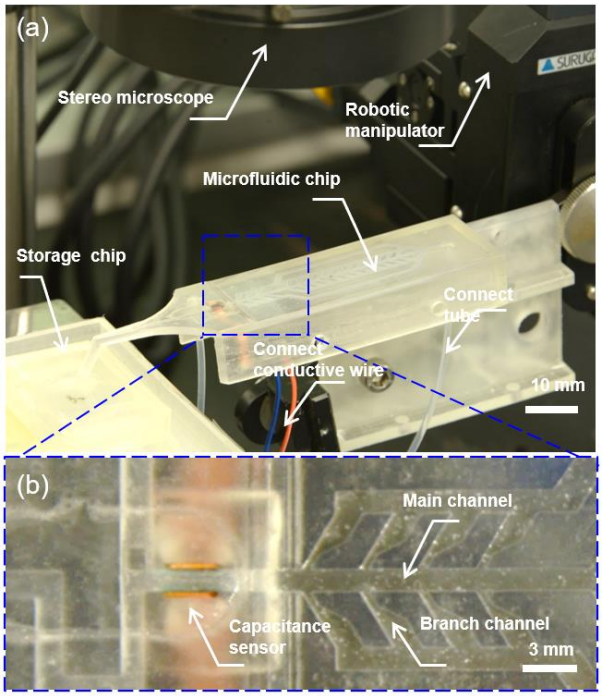

Fig. 3. A photograph of the experimental system. (a) System setup. (b) Microfluidic chip with a capacitive sensor.

main channel. Thus, the flow in the main channel also increases from the back to the front direction. The velocity increases in the main channel. To confirm the velocity effect, we conducted a finite element analysis using COMSOL software. The velocity distribution in the microfluidic chip is shown in Fig. 2(b). Fig. 2(c) shows the velocity of the center line of the main channel. It demonstrated the design structure had a step-increasing velocity property. By dividing the branch channel into two parts, the increase in velocity was more obvious in the second part of the main channel.

B. Capacitive Sensor for detecting oocytes

It is important to detect a single oocyte in the system for robotic manipulation. To control the oocyte release process using the movable microfluidic chip, the number of oocytes is a key factor. Due to the large movement range of the microfluidic chip, oocytes are not easily tracked using traditional visual images. Therefore, a capacitive sensor is employed to achieve precise single oocyte release since it can be installed into movable objects. Two plate electrodes are placed on two oppositive sidewalls of the channel to form the capacitive sensor. A high-frequency voltage is applied to the pair electrode [28]. In this case, the voltage and frequency are set to 5 V and 100 kHz, respectively. The capacitance relates to the relatively effective permittivity of the medium between two plate electrodes. By changing the permittivity, the capacitance also changes.

In the experiment, the medium was a Barth's buffer solution in the initial state. It mainly contains NaCl, HEPES, KCl, $Ca(NO_3)_2$, $CaCl_2$, $MgSO_4$, and $NaHCO_3$. When oocytes moved in the channel to the middle of the capacitive sensor, the medium contained oocytes and buffer solution. It formed a composite medium. Thus, the value of effective permittivity changed. The capacitance also changed and was detected by

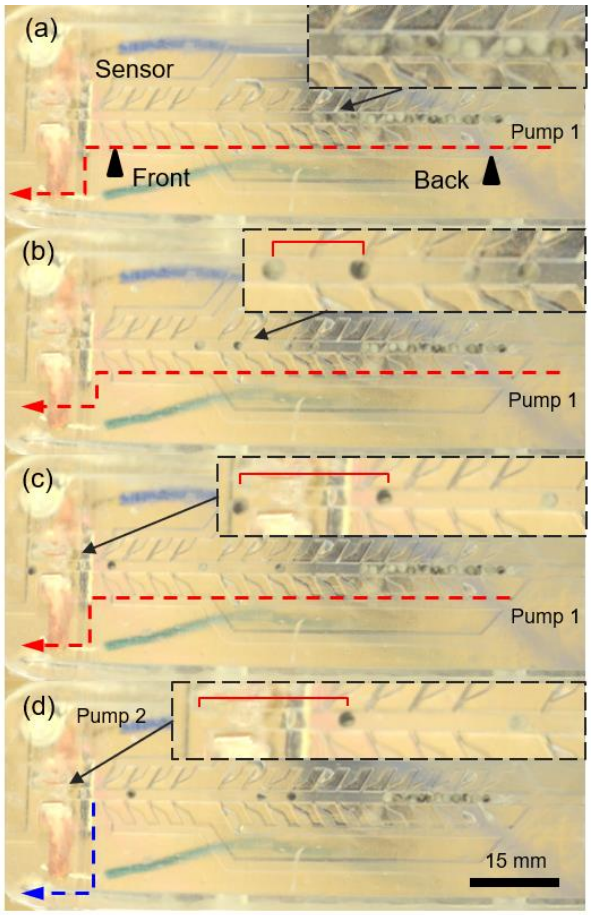

Fig. 4. A gap effect between oocytes in a microfluidic chip. (a) Initial state. (b) Starting to generate a gap between oocytes. (c) Increasing the distance of the gap. (d) Releasing the first oocyte in the channel.

an external monitor. To achieve the release of single oocytes from the pipette tip, the capacitance sensor detects whether oocytes have passed or not. When different numbers of oocytes reached the sensor position, the number of oocytes was counted. Here, the width of each electrode is 3 mm, the distance between two electrodes is 1.6 mm, the effect height is 1.6 mm, and the electrode is made of copper. Currently, copper is selected to test the detection function. In order to avoid the material affecting the oocyte, we will change the electrode material in the future. In this case, the capacitive sensor was selected for the movable microfluidic chip because it can sense oocytes at high speed without using a camera image. Furthermore, it was not easy for cameras to observe the moving oocyte on a movable microfluidic chip.

C. System Setup

A conceptual image of a movable microfluidic chip is shown in Fig. 1. It is configured with a movable observer part, as shown in Fig. 3(a). The movable microfluidic chip part is a microfluidic chip integrated in the 3DoF-robot manipulator (Micromanipulator MC104, Micro Support Co., Ltd., Japan). The sensor is set at the front of the channel, as shown in Fig. 3(b). A LCR meter (ZM2372, NF Techno Commerce Co., Ltd., Japan) was applied to collect the sensor signal. The microfluidic chip with a pipette tip shape was directly fabricated using a 3D printer (Form 3+, Formlabs Inc., USA).

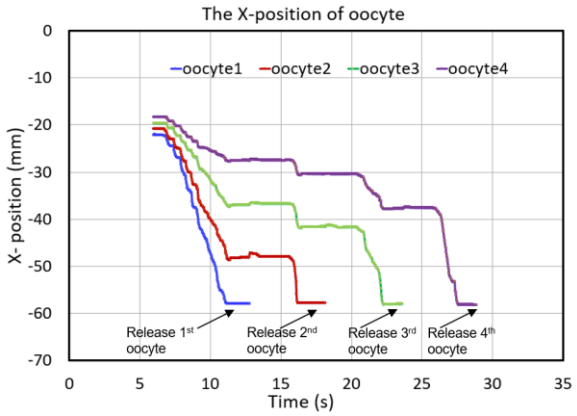

Fig. 5. The x-position of the first 4 oocytes when flowing out.

The storage chip part was held by a 3axis stage for manipulating oocyte. It was also fabricated by 3D printing. The size of the trapping hole is 1.6 mm in diameter and 1.6 mm in depth, respectively. The pump control part had two syringe pumps (KDS 230, KD Scientific Inc., USA). One pump was used to control the flow in the main channel to generate a gap effect. The other pump was utilized to push out a single oocyte after the first oocyte reached the target position. The oocytes were observed by a stereo microscope (LEICA MZ16F, Leica Microsystems Ltd., Germany) which equipped with a CCD camera (Basler acA1300-200uc, Basler AG, Germany). The real-time information on the release process was displayed on the monitor. The sensor signals were applied to operate the pump. Image analysis was exploited to confirm the oocyte position. Each pump and robotic manipulator were controlled using a PC program.

III. Experiment and Results

A. Gap Effect between Oocytes in the channel

We first evaluated the movable microfluidic chip capable of releasing a single oocyte. *Xenopus* oocytes, with a diameter of about 1.2 mm, were used in this manipulation. The results of the manipulation of oocytes are shown in Fig. 4 (see supplied video). Firstly, oocytes were stored in the main channel for transportation and manipulation, as shown in Fig. 4(a). Then, pump 1 controlled oocytes to move from the back side to the front side in the main channel, and a gap effect was generated in the moving process, as shown in Fig. 4(b). Generally, the first few oocytes in the front started to move first, and the remaining oocytes were left at the back of the channel. It was because the oocytes stayed in the channel causing a large flow resistance. The solution flowed into the side channel and then converged to the front of oocytes queue through the branch channel. The distance of the gap increased when oocytes moved to the tip of the main channel, as shown in Fig. 4(c). Fig. 5 shows the movement position of the first 4 oocytes during the manipulation. When the first oocyte reached the target position, the gap distance can reach around 19.34 mm, which was approximately 16 times the diameter of the oocyte. When the first oocyte in the queue reached the target position, pump 1 was stopped, and oocytes kept in their current position. Finally, the first oocyte was pushed out from the pipette tip of the microfluidic chip using pump 2, as shown

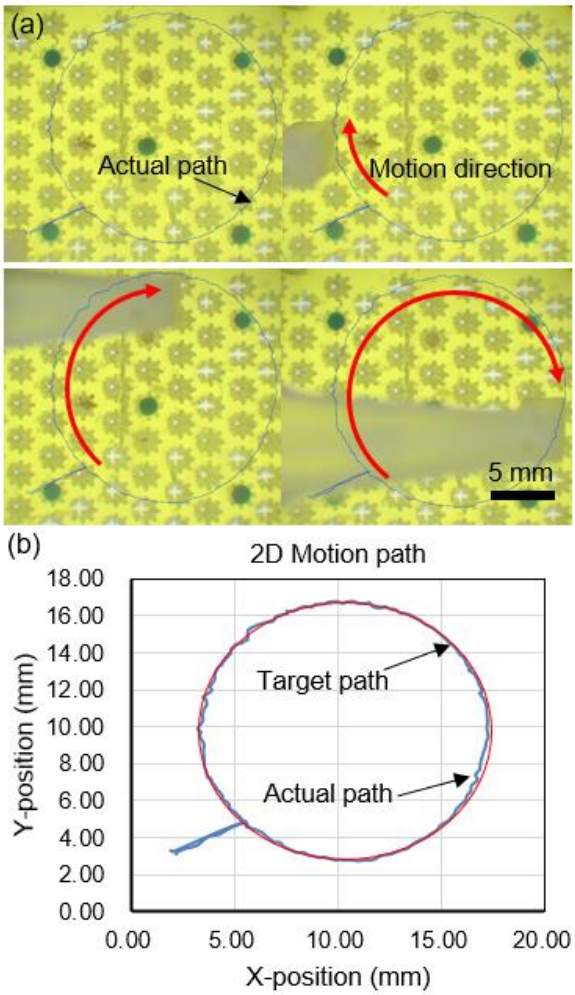

Fig. 6. The movement of the tip of a movable microfluidic chip. (a) The movement of the tip along a circle trajectory. (b) Comparison of the trajectory between the target and the actual path.

in Fig. 4(d). We repeated the process until all oocytes were released one by one. The isolation success rate was around 87.14% during the seven release experiments of 20 oocytes. Compared with manual isolation [29] and microfluidic chip trapping oocytes [30], this method achieved multiple oocytes separation. In this manipulation, the oocytes only moved in the main channel and did not meet any obstacles. Therefore, there was no deformation in the shape of the oocytes. In some cases, if the oocytes were squeezed too tightly when they were sucked into the main channel, oocytes may not be easily separated in one step. It required repeating the sucking-ejecting process about 3 times in the main channel. This process can reduce the contact force between two oocytes. Thus, the gap effect was easier to generate between oocytes. The additional step ensured the successful release of a single oocyte.

B. Motion of the tip of the movable microfluidic chip

We confirmed the tip position accuracy of the microfluidic chip integrated into the 3DoF-robot manipulator. The robotic manipulator moved along a circular trajectory at a constant velocity. The tip position was measured by a CCD camera installed on the stereo microscope. Fig. 6 shows movement of

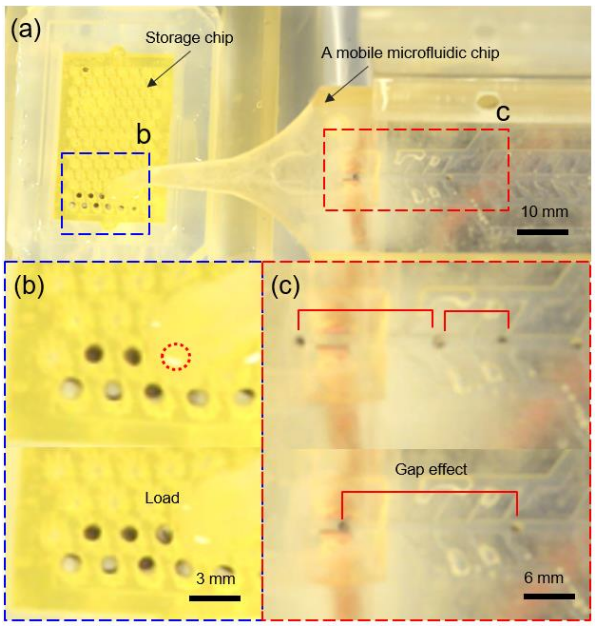

Fig. 7. Loading of oocytes using the movable microfluidic chip. (a) Loading oocytes one by one. (b) Loading results. (c) Gap effect when loading single oocytes.

the tip of a movable microfluidic chip (see supplied video). Here, within the maximum viewing area, the diameter of the circular target trajectory was set to 6.8 mm. The drive velocity of the robotic manipulator was 0.5 mm/s in the *x*–*y* direction. The actual trajectory of the tip position was measured at 100 points, as shown in Fig. 6(b). Thus, the maximum error between the actual tip position and the target trajectory position was approximately 0.34 mm. In this case, the total error of position accuracy included tip position error and measurement error. The measurement error depended on the pixel resolution of the CCD camera. The single pixel of the display was 29.2 μm. Therefore, the measurement error was around 0.06 mm. The tip position error can be calculated using the root-mean-square error, expressed as [31]:

$$e_{tip} = \sqrt{e_{total}^2 - e_{measure}^2} \tag{5}$$

Where, e_{tip} is the tip position error, e_{total} is the total error, and $e_{measure}$ is the measuring error. Thus, the tip position error was around 0.33 mm. This value is 5 times smaller than the trapping well diameter. Currently, it meets the requirement of controlling the movable microfluidic chip to the well position. The accuracy of the tip position will further be used to select the motion path.

On the other hand, the highest position accuracy was determined by the robotic manipulator due to the microfluidic chip was fixed to the manipulator. When the speed of the manipulator increased, the total position error of the tip increased. It was because the manipulator divided the non-linear path into many x-y linear steps. In fact, a movable microfluidic chip was formed when the microfluidic chip was integrated into the 3DoF robot manipulator. The positional accuracy of the microfluidic chip tip should be close to that of a robot manipulator. The working range of the movable microfluidic chip was also determined by the manipulator.

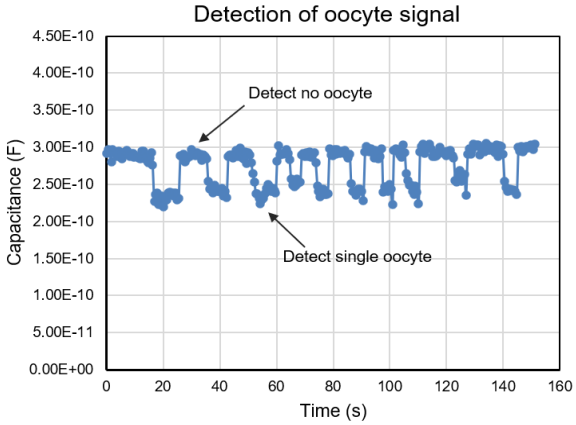

Fig. 8. The detection of oocyte capacitance signals during loading.

C. *Application to Load Oocytes*

We performed an experiment to demonstrate the ability to manipulate oocytes using a movable microfluidic chip. Fig. 7 shows the results of the manipulating process (see supplied video). Firstly, the position of the system was calibrated. Then, the pipette tip of the microfluidic chip was moved to the target position on the storage chip, as shown in Fig. 7(b). Next, by controlling pump 1, the oocyte in the main channel was separated, and a gap effect was generated, as shown in Fig. 7(c). When the first oocyte passed through the sensor position and reached the release position, the capacitance sensor can detect a signal, as shown in Fig. 8. Once receiving the signal, pump 1 was stopped to prevent the release of multiple oocytes. Meanwhile, the sensor can be utilized to count the number of oocytes. Although some bubbles are present in the side channels, they remain in front of the side channels during the release process. Thus, the sensor is not disturbed by air bubbles. These bubbles will be eliminated through other channel designs in the future. Finally, the first oocyte was pushed out of the microfluidic chip into the storage chip using pump 2. By repeating this process, all oocytes in the channel can be manipulated one by one. When loading a single oocyte into the storage chip, the flow speed of pump 2 should not be fast. Here, speed is set to 2 ml/min. Otherwise, oocytes were susceptible to damage due to the high impact force at the trapping well of the storage chip. Moreover, the high-speed flow can influence the loaded oocyte near the target location because of the small distance between the two trapping wells. The CCD camera was used to observe the manipulation process in real-time. The manipulation of oocytes demonstrated the capability of the movable microfluidic chip that can more flexibly achieve cell manipulation. In near future work, we will develop a full automation cell process with image analysis and sensor detection. Thus, the cell processing system can be placed in a closed biological environment to avoid contamination.

IV. Conclusion and Future Work

In this study, we presented a movable microfluidic chip for cell manipulation. The microfluidic chip can release a single cell through the gap effect between oocytes in the channel. The theoretical model was analyzed by simulating the flow

distribution of the microfluidic chip. In the main channel, the velocity step increased from the back side to the front side. Unlike conventional microfluidic chips, a pipette tip was fabricated directly on the chip using 3D printing. Then, the microfluidic chip was integrated into a robotic manipulator. The result of the tip position accuracy of the movable microfluidic ship was around 0.33 mm. The robotic manipulator determined the highest positioning accuracy of the tip and working range. *Xenopus* oocytes were used for manipulation. Utilizing the gap effect, the oocytes were not deformed in shape in the manipulation process. The gap distance can reach approximately 16 times the diameter of the oocyte. Moreover, a capacitive sensor in the microfluidic chip can detect a single oocyte. The width of the electrode was required to be larger than 2 times the diameter of the oocyte. Finally, with the construction system, we demonstrated the loading of a single oocyte into a storage chip using the movable microfluidic chip. From these results, we confirmed that the movable microfluidic chip can be applied for cell manipulation processes. The proposed method will contribute to the fields of bioengineering and micromanipulation. In our future work, we will establish a fully automated cell manipulation system with image deep learning models and sensor detection signals.

REFERENCES

[1] J. J. Tyson and B. Novak, "Control of cell growth, division and death: information processing in living cells," *Interface Focus*, vol. 4, no. 3, p. 20130070, Jun. 2014, doi: 10.1098/rsfs.2013.0070.

[2] L. Li, K. Chen, Y. Wu, G. Xiang, and X. Liu, "Epigenome-Metabolome-Epigenome signaling cascade in cell biological processes," *J. Genet. Genomics*, vol. 49, no. 4, pp. 279–286, Apr. 2022, doi: 10.1016/j.jgg.2021.09.006.

[3] L. Liu, D. Chen, J. Wang, and J. Chen, "Advances of Single-Cell Protein Analysis," *Cells*, vol. 9, no. 5, p. 1271, May 2020, doi: 10.3390/cells9051271.

[4] D. Irimia, "Manipulating Cells, Techniques," in *Encyclopedia of Microfluidics and Nanofluidics*, D. Li, Ed., Boston, MA: Springer US, 2008, pp. 1048–1050. doi: 10.1007/978-0-387-48998-8_851.

[5] A. Shakoor, W. Gao, L. Zhao, Z. Jiang, and D. Sun, "Advanced tools and methods for single-cell surgery," *Microsyst. Nanoeng.*, vol. 8, no. 1, Art. no. 1, Apr. 2022, doi: 10.1038/s41378-022-00376-0.

[6] Y. Dai *et al.*, "Precise Control of Customized Macrophage Cell Robot for Targeted Therapy of Solid Tumors with Minimal Invasion," *Small*, vol. 17, no. 41, p. 2103986, Oct. 2021, doi: 10.1002/smll.202103986.

[7] B. Song, W. Zhang, X. Bai, L. Feng, D. Zhang, and F. Arai, "A novel portable cell sonoporation device based on open-source acoustofluidics," in *2020 IEEE/RSJ International Conference on Intelligent Robots and Systems (IROS)*, Las Vegas, NV, USA: IEEE, Oct. 2020, pp. 2786–2791. doi: 10.1109/IROS45743.2020.9341603.

[8] F. Arai, C. Ng, H. Maruyama, A. Ichikawa, H. El-Shimy, and T. Fukuda, "On chip single-cell separation and immobilization using optical tweezers and thermosensitive hydrogel," *Lab. Chip*, vol. 5, no. 12, p. 1399, 2005, doi: 10.1039/b502546j.

[9] M. Hagiwara, T. Kawahara, T. Iijima, and F. Arai, "High-Speed Magnetic Microrobot Actuation in a Microfluidic Chip by a Fine V-Groove Surface," *IEEE Trans. Robot.*, vol. 29, no. 2, pp. 363–372, Apr. 2013, doi: 10.1109/TRO.2012.2228310.

[10] S. Sakuma, K. Nakahara, and F. Arai, "Continuous Mechanical Indexing of Single-Cell Spheroids Using a Robot-Integrated Microfluidic Chip," *IEEE Robot. Autom. Lett.*, vol. 4, no. 3, pp. 2973–2980, Jul. 2019, doi: 10.1109/LRA.2019.2923976.

[11] W. Yu *et al.*, "A ferrobotic system for automated microfluidic logistics," *Sci. Robot.*, vol. 5, no. 39, p. eaba4411, Feb. 2020, doi: 10.1126/scirobotics.aba4411.

[12] C. Dai *et al.*, "Robotic Manipulation of Deformable Cells for Orientation Control," *IEEE Trans. Robot.*, vol. 36, no. 1, pp. 271–283, Feb. 2020, doi: 10.1109/TRO.2019.2946746.

[13] B. Turan *et al.*, "Detection and Control of Air Liquid Interface with an Open-Channel Microfluidic Chip for Circulating Tumor Cells Isolation from Human Whole Blood," *IEEE Robot. Autom. Lett.*, pp. 1–1, 2020, doi: 10.1109/LRA.2020.3007476.

[14] Y. Zhao *et al.*, "Microfluidic Actuated and Controlled Systems and Application for Lab-on-Chip in Space Life Science," *Space Sci. Technol.*, vol. 3, p. 0008, Jan. 2023, doi: 10.34133/space.0008.

[15] T. W. Murphy, Q. Zhang, L. B. Naler, S. Ma, and C. Lu, "Recent advances in the use of microfluidic technologies for single cell analysis," *The Analyst*, vol. 143, no. 1, pp. 60–80, 2018, doi: 10.1039/C7AN01346A.

[16] B. Deng, H. Wang, Z. Tan, and Y. Quan, "Microfluidic Cell Trapping for Single-Cell Analysis," *Micromachines*, vol. 10, no. 6, Art. no. 6, Jun. 2019, doi: 10.3390/mi10060409.

[17] N. Xiang, J. Wang, Q. Li, Y. Han, D. Huang, and Z. Ni, "Precise Size-Based Cell Separation via the Coupling of Inertial Microfluidics and Deterministic Lateral Displacement," *Anal. Chem.*, vol. 91, no. 15, pp. 10328–10334, Aug. 2019, doi: 10.1021/acs.analchem.9b02863.

[18] M. Darboui, R. Askari Moghadam, and R. Parichehr, "Microfluidics chip inspired by fish gills for blood cells and serum separation," *Sens. Actuators Phys.*, vol. 346, p. 113839, Oct. 2022, doi: 10.1016/j.sna.2022.113839.

[19] L. Mazutis, J. Gilbert, W. L. Ung, D. A. Weitz, A. D. Griffiths, and J. A. Heyman, "Single-cell analysis and sorting using droplet-based microfluidics," *Nat. Protoc.*, vol. 8, no. 5, Art. no. 5, May 2013, doi: 10.1038/nprot.2013.046.

[20] S. Liang *et al.*, "Interaction between positive and negative dielectric microparticles/microorganism in optoelectronic tweezers," *Lab. Chip*, vol. 21, no. 22, pp. 4379–4389, 2021, doi: 10.1039/D1LC00610J.

[21] D. Lv *et al.*, "Trapping and releasing of single microparticles and cells in a microfluidic chip," *ELECTROPHORESIS*, vol. 43, no. 21–22, pp. 2165–2174, 2022, doi: 10.1002/elps.202200091.

[22] Y. Kasai *et al.*, "Breakthrough in purification of fossil pollen for dating of sediments by a new large-particle on-chip sorter," *Sci. Adv.*, vol. 7, no. 16, p. eabe7327, Apr. 2021, doi: 10.1126/sciadv.abe7327.

[23] S. Liang *et al.*, "A Versatile Optoelectronic Tweezer System for Micro-Objects Manipulation: Transportation, Patterning, Sorting, Rotating and Storage," *Micromachines*, vol. 12, no. 3, p. 271, Mar. 2021, doi: 10.3390/mi12030271.

[24] K. Hiramatsu *et al.*, "High-throughput label-free molecular fingerprinting flow cytometry," *Sci. Adv.*, vol. 5, no. 1, p. eaau0241, Jan. 2019, doi: 10.1126/sciadv.aau0241.

[25] M. Bayareh, "An updated review on particle separation in passive microfluidic devices," *Chem. Eng. Process. - Process Intensif.*, vol. 153, p. 107984, Jul. 2020, doi: 10.1016/j.cep.2020.107984.

[26] K. W. Oh, K. Lee, B. Ahn, and E. P. Furlani, "Design of pressure-driven microfluidic networks using electric circuit analogy," *Lab Chip*, vol. 12, no. 3, pp. 515–545, 2012, doi: 10.1039/C2LC20799K.

[27] J. Chen *et al.*, "Sorting of circulating tumor cells based on the microfluidic device of a biomimetic splenic interendothelial slit array," *Microfluid. Nanofluidics*, vol. 25, no. 7, p. 57, Jul. 2021, doi: 10.1007/s10404-021-02459-2.

[28] S. Amaya, H. Sugiura, B. Turan, S. Kaneko, and F. Arai, "A Pipette Tip Integrated with a Capacitive Microsensor Fabricated by Combined 3D Printing and MEMS Process for Cell Detection and Transportation," in *2023 IEEE 36th International Conference on Micro Electro Mechanical Systems (MEMS)*, Jan. 2023, pp. 57–60. doi: 10.1109/MEMS49605.2023.10052499.

[29] K. L. Mowry, "Using the Xenopus Oocyte Toolbox," *Cold Spring Harb. Protoc.*, vol. 2020, no. 4, p. pdb.top095844, Apr. 2020, doi: 10.1101/pdb.top095844.

[30] I. Baburin, S. Beyl, and S. Hering, "Automated fast perfusion of Xenopus oocytes for drug screening," *Pflüg. Arch.*, vol. 453, no. 1, pp. 117–123, Oct. 2006, doi: 10.1007/s00424-006-0125-y.

[31] M. Hagiwara, T. Kawahara, Y. Yamanishi, T. Masuda, L. Feng, and F. Arai, "On-chip magnetically actuated robot with ultrasonic vibration for single cell manipulations," *Lab. Chip*, vol. 11, no. 12, pp. 2049–2054, 2011, doi: 10.1039/C1LC20164F.